

Optimal time-complexity speed planning for robot manipulators

Luca Consolini¹, Marco Locatelli¹, Andrea Minari¹, Ákos Nagy², István Vajk²

¹ Dipartimento di Ingegneria e Architettura, University of Parma, Italy

² Department of Automation and Applied Informatics, Budapest University of Technology and Economics, Hungary

February 2018

Abstract

We consider the speed planning problem for a robotic manipulator. In particular, we present an algorithm for finding the time-optimal speed law along an assigned path that satisfies velocity and acceleration constraints and respects the maximum forces and torques allowed by the actuators. The addressed optimization problem is a finite dimensional reformulation of the continuous-time speed optimization problem, obtained by discretizing the speed profile with N points. The proposed algorithm has linear complexity with respect to N and to the number of degrees of freedom. Such complexity is the best possible for this problem. Numerical tests show that the proposed algorithm is significantly faster than algorithms already existing in literature.

Index terms— time-optimal control, motion planning, robot manipulator

1 Introduction

For robotic manipulators, the motion planning problem is often decomposed into two sub-problems: path planning and speed planning [10].

The first problem consists in finding a path (i.e., the curve followed by the joints) that joins assigned initial and final positions. The second problem consists in finding the time-optimal speed law along the path that satisfies assigned velocity and acceleration constraints and respects the maximum forces and torques allowed by the actuators. In this paper we consider only the second problem. Namely, given a path Γ in the robot configuration space, we want to find the optimal speed-law that allows following Γ while satisfying assigned kinematic and dynamics constraints. More specifically, we consider the problem

$$\begin{aligned} \min_{\mathbf{q}, \boldsymbol{\tau}} \quad & t_f \\ & \mathbf{D}(\mathbf{q})\ddot{\mathbf{q}} + \mathbf{C}(\mathbf{q}, \dot{\mathbf{q}})\dot{\mathbf{q}} + \boldsymbol{\ell}(\mathbf{q}) = \boldsymbol{\tau}, \\ & (\dot{\mathbf{q}}^2, \ddot{\mathbf{q}}, \boldsymbol{\tau}) \in \mathcal{C}(\mathbf{q}), \\ & \mathbf{q} \in \Gamma, \end{aligned} \tag{1}$$

where: t_f is the travel time; \mathbf{q} is the generalized position; $\boldsymbol{\tau}$ is the generalized force vector; $\mathbf{D}(\mathbf{q})$ is the mass matrix; $\mathbf{C}(\mathbf{q}, \dot{\mathbf{q}})$ is a matrix accounting for centrifugal and Coriolis effects; $\boldsymbol{\ell}(\mathbf{q})$ is an external force term (for instance gravity); $\mathcal{C}(\mathbf{q})$ is a set that represents the kinematic and dynamic limitations of the manipulator.

1.1 Related Works

There are mainly three different families of speed profile generation methods: *Numerical Integration*, *Dynamic Programming*, and *Convex Optimization*.

References [1, 18] are among the first works that study Problem 1 using the *Numerical Integration* approach. In particular, they find the time-optimal speed law *as a function of arc-length* and not as a function of time. This choice simplifies the mathematical structure of the resulting problem and has been adopted by most of successive works. In [1, 18] the optimization problem is solved with iterative algorithms. In particular, reference [1] finds the points in which the acceleration changes sign using the numerical integration of the second order differential equations representing the motions obtained with the maximum and minimum possible accelerations. Reference [18] is based on geometrical considerations on the feasible set. However, this approach has some limitations due to the determination of the *switching points* that is the main source of failure of this approach (see [26, 23]). For recent results on *Numerical Integration* see [20, 21, 22]. For instance [22] considers the case of redundant manipulators.

In the *Dynamic Programming* approach the problem is solved with a finite element approximation of the Hamilton-Jacobi-Bellman equation (see [24, 25, 17]). The main difficulty with this approach is the high computational time due to the need of solving a problem with a large number of variables.

The *Convex Optimization* approach is based on the approximation of Problem (1) with a finite dimensional optimization problem obtained through spatial discretization. Reference [27] is one of the early works using this approach. It shows that Problem (1) becomes convex after a change of variables and that a discretized version of Problem (1) is a *Second-Order Cone Programming* (SOCP) problem. This approach has the advantage that the optimization problem can be tackled with available solvers (e.g., see [11, 8]). Moreover, differently from the *Numerical Integration*, this approach allows considering other convex objective functions. However, the convex programming approach could be inappropriate (see for instance [20]) for online motion planning since the computational time grows rapidly (even if still polynomially) with respect to the number of samples in the discretized problem. Subsequent works, starting from [27], extend the applicability of this approach to different scenarios (see [6, 5]) and propose algorithms that reduce the computational time (see [9, 16]). To reduce computational time, reference [9] proposes an approach based on *Sequential Linear Programming* (SLP). Namely, the algorithm proposed in [9] sequentially linearizes the objective function around the current point, while a trust region method ensures the convergence of the process. Further, [16] shows that, using a suitable discretization method, the time optimal velocity profile can be obtained by *Linear Programming* (LP) with the benefit of a lower computation time with respect to convex solvers.

A very recent, and very interesting, paper, closely related to our work, is [19]. In Section 4.1, we will shortly describe the approach proposed there and compare it with our approach.

Our approach combines the ideas which we previously proposed in two other works. Namely, in [3] we proposed an exact linear-time forward-backward algorithm for the solution of a velocity planning problem for a vehicle over a given trajectory under velocity, normal and tangential acceleration bounds. In [5], a method based on the sequential solution of two-dimensional subproblems is proposed for the solution of the so-called waiter motion problem. The method is able to return a feasible, though not necessarily optimal, solution. In the cur-

rent paper we merge the ideas proposed in the two above mentioned papers in order to derive an approach for the speed planning of robotic manipulators. This will be proved to return an optimal solution and to have linear time complexity both with respect to the number of discretization points and to the number of degrees of freedom of the robotic manipulator.

1.2 Main results

The purpose of this paper is to provide a speed planning method for robotic manipulators with optimal time complexity. With respect to the existing literature, the new contributions of this work are the following ones.

- We propose a new algorithm for solving a finite dimensional reformulation of Problem (1) obtained with N discretization points.
- We show that if set $\mathcal{C}(\mathbf{q})$ in Problem (1) is defined by linear constraints, then the proposed algorithm has complexity $O(pN)$, where N is the number of discretization points and p is the number of degrees of freedom. Moreover, such complexity is optimal.
- By numerical tests, we show that the proposed procedure is significantly faster than algorithms already existing in literature.

1.3 Paper Organization

In Section 2, we present the time-optimal control problem for robotic manipulators in continuous time. In Section 3, we present a class of optimization problems and an exact solution algorithm. We prove the correctness of the algorithm and compute its time complexity, showing that such complexity is optimal in case of linear constraints. In Section 4, we show that by suitably discretizing the continuous time problem, it is possible to obtain a finite dimensional problem with linear constraints that falls into the class defined in Section 3. Finally, we present an experiment for a 6-DOF industrial robotic manipulator and we compare the performance of the proposed approach with that of existing solvers (see [11, 8, 16]).

1.4 Notation

We denote with \mathbb{R}_+ the set of nonnegative real numbers. For a vector $\mathbf{x} \in \mathbb{R}^n$, $|\mathbf{x}| \in \mathbb{R}_+^n$ denotes the component-wise absolute value of \mathbf{x} and we define the norms $\|\mathbf{x}\|_2 := \sqrt{\sum_{i=1}^n |x_i|^2}$, $\|\mathbf{x}\|_\infty := \max\{|x_1|, \dots, |x_n|\}$. We also set $\mathbf{1} = [1 \dots 1]^T$.

For $r \in \mathbb{N}$, we denote by $C^r([a, b], \mathbb{R}^n)$ the set of continuous functions from $[a, b] \subset \mathbb{R}$ to \mathbb{R}^n that have continuous first r derivatives. For $f \in C^1([a, b], \mathbb{R})$, f' denotes the derivative and notation \dot{f} is used if f is a function of time. We set $\|\mathbf{f}\|_\infty := \sup_{i=1, \dots, n} \sup\{|f_i(x)| : x \in [a, b]\}$. We say that $\mathbf{f} : [a, b] \rightarrow \mathbb{R}^n$ is bounded if there exists $M \in \mathbb{R}$ such that $\|\mathbf{f}(x)\|_\infty \leq M$.

Consider $h, g : \mathbb{N} \rightarrow \mathbb{R}$. We say that $h(n) = O(g(n))$, if there exists a positive constant M such that, for all sufficiently large values of n , $|h(n)| \leq M|g(n)|$.

2 Problem formulation

Let \mathcal{Q} be a smooth manifold of dimension p that represents the configuration space of a robotic manipulator with p -degrees of freedom (p -DOF). Let $\Gamma : [0, 1] \rightarrow \mathcal{Q}$ be a smooth

curve whose image set $\text{Im } \Gamma$ represents the assigned path to be followed by the manipulator. We assume that there exist two open sets $U \supset \text{Im } \Gamma$, $V \subset \mathbb{R}^p$ and an invertible and smooth function $\phi : U \rightarrow V$. Function ϕ is a local chart that allows representing each configuration $q \in U$ with coordinate vector $\phi(q) \in \mathbb{R}^p$.

The coordinate vector \mathbf{q} of a trajectory in U satisfies the dynamic equation

$$\mathbf{D}(\mathbf{q})\ddot{\mathbf{q}} + \mathbf{C}(\mathbf{q}, \dot{\mathbf{q}})\dot{\mathbf{q}} + \boldsymbol{\ell}(\mathbf{q}) = \boldsymbol{\tau}, \quad (2)$$

where $\mathbf{q} \in \mathbb{R}^p$ is the generalized position vector, $\boldsymbol{\tau} \in \mathbb{R}^p$ is the generalized force vector, $\mathbf{D}(\mathbf{q})$ is the mass matrix, $\mathbf{C}(\mathbf{q}, \dot{\mathbf{q}})$ is the matrix accounting for centrifugal and Coriolis effects (assumed to be linear in $\dot{\mathbf{q}}$) and $\boldsymbol{\ell}(\mathbf{q})$ is the vector accounting for joints position dependent forces, including gravity. Note that we do not consider Coulomb friction forces.

Let $\boldsymbol{\gamma} \in C^2([0, s_f], \mathbb{R}^p)$ be a function such that $\phi(\boldsymbol{\gamma}[0, s_f]) = \text{Im } \Gamma$ and $(\forall \lambda \in [0, s_f]) \|\boldsymbol{\gamma}'(\lambda)\| = 1$. The image set $\boldsymbol{\gamma}([0, s_f])$ represents the coordinates of the elements of reference path Γ . In particular, $\boldsymbol{\gamma}(0)$ and $\boldsymbol{\gamma}(s_f)$ are the coordinates of the initial and final configurations. Define t_f as the time when the robot reaches the end of the path. Let $\lambda : [0, t_f] \rightarrow [0, s_f]$ be a differentiable monotone increasing function that represents the position of the robot as a function of time and let $v : [0, s_f] \rightarrow [0, +\infty]$ be such that $(\forall t \in [0, t_f]) \dot{\lambda}(t) = v(\lambda(t))$. Namely, $v(s)$ is the velocity of the robot at position s . We impose $(\forall s \in [0, s_f]) v(s) \geq 0$. For any $t \in [0, t_f]$, using the chain rule, we obtain

$$\begin{aligned} \mathbf{q}(t) &= \boldsymbol{\gamma}(\lambda(t)), \\ \dot{\mathbf{q}}(t) &= \boldsymbol{\gamma}'(\lambda(t))v(\lambda(t)), \\ \ddot{\mathbf{q}}(t) &= \boldsymbol{\gamma}'(\lambda(t))v'(\lambda(t))v(\lambda(t)) + \boldsymbol{\gamma}''(\lambda(t))v(\lambda(t))^2. \end{aligned} \quad (3)$$

Substituting (3) into the dynamic equations (2) and setting $s = \lambda(t)$, we rewrite the dynamic equation (2) as follows:

$$\mathbf{d}(s)v'(s)v(s) + \mathbf{c}(s)v(s)^2 + \mathbf{g}(s) = \boldsymbol{\tau}(s), \quad (4)$$

where the parameters in (4) are defined as

$$\begin{aligned} \mathbf{d}(s) &= \mathbf{D}(\boldsymbol{\gamma}(s))\boldsymbol{\gamma}'(s), \\ \mathbf{c}(s) &= \mathbf{D}(\boldsymbol{\gamma}(s))\boldsymbol{\gamma}''(s) + \mathbf{C}(\boldsymbol{\gamma}(s), \boldsymbol{\gamma}'(s))\boldsymbol{\gamma}'(s), \\ \mathbf{g}(s) &= \boldsymbol{\ell}(\boldsymbol{\gamma}(s)). \end{aligned} \quad (5)$$

The objective function is given by the overall travel time t_f defined as

$$t_f = \int_0^{t_f} 1 \, dt = \int_0^{s_f} v(s)^{-1} \, ds. \quad (6)$$

Let $\boldsymbol{\mu}, \boldsymbol{\psi}, \boldsymbol{\alpha} : [0, s_f] \rightarrow \mathbb{R}_+^p$ be assigned bounded functions and consider the following minimum time problem:

Problem 1.

$$\min_{v \in C^1, \boldsymbol{\tau} \in C^0} \int_0^{s_f} v(s)^{-1} ds, \quad (7)$$

subject to $(\forall s \in [0, s_f])$

$$\mathbf{d}(s)v'(s)v(s) + \mathbf{c}(s)v(s)^2 + \mathbf{g}(s) = \boldsymbol{\tau}(s), \quad (8)$$

$$\boldsymbol{\gamma}'(s)v(s) = \dot{\mathbf{q}}(s), \quad (9)$$

$$\boldsymbol{\gamma}'(s)v'(s)v(s) + \boldsymbol{\gamma}''v(s)^2 = \ddot{\mathbf{q}}(s), \quad (10)$$

$$|\boldsymbol{\tau}(s)| \leq \boldsymbol{\mu}(s), \quad (11)$$

$$|\dot{\mathbf{q}}(s)| \leq \boldsymbol{\psi}(s), \quad (12)$$

$$|\ddot{\mathbf{q}}(s)| \leq \boldsymbol{\alpha}(s), \quad (13)$$

$$v(s) \geq 0, \quad (14)$$

$$v(0) = 0, v(s_f) = 0, \quad (15)$$

where (8) represents the robot dynamics, (9)-(10) represent the relation between the path $\boldsymbol{\gamma}$ and the generalized position q shown in (3), (11) represents the bounds on generalized forces, (12) and (13) represent the bounds on joints velocity and acceleration. Constraints (15) specify the interpolation conditions at the beginning and at the end of the path.

The following assumption is a basic requirement for fulfilling constraint (12).

Assumption 1. *We assume that $\boldsymbol{\psi}$ is a positive continuous function, i.e., $(\forall s \in [0, s_f]) \psi_i(s) > 0$ with $i = 1, \dots, p$.*

Next assumption requires that the maximum allowed generalized forces are able to counteract external forces (such as gravity) when the manipulator is fixed at each point of Γ .

Assumption 2. *We assume that $\exists \varepsilon \in \mathbb{R}, \varepsilon > 0$ such that $(\forall s \in [0, s_f]) \boldsymbol{\mu}(s) - |\mathbf{g}(s)| > \varepsilon \mathbf{1}$.*

In fact for $v = 0$ condition (11) reduces to $(\forall s \in [0, s_f]) |\mathbf{g}(s)| \leq \boldsymbol{\mu}(s)$.

Problem 1 is nonconvex, but it becomes convex after a simple change of variables (as previously noted in [27]). Indeed, $(\forall s \in [0, s_f])$ set

$$a(s) = v'(s)v(s), \quad b(s) = v(s)^2, \quad (16)$$

and note that

$$b'(s) = 2a(s). \quad (17)$$

Then, Problem 1 becomes:

Problem 2.

$$\min_{a, \tau \in C^0, b \in C^1} \int_0^{s_f} b(s)^{-1/2} ds, \quad (18)$$

subject to $(\forall s \in [0, s_f])$

$$\mathbf{d}(s)a(s) + \mathbf{c}(s)b(s) + \mathbf{g}(s) = \boldsymbol{\tau}(s), \quad (19)$$

$$\boldsymbol{\gamma}'(s)a(s) + \boldsymbol{\gamma}''(s)b(s) = \ddot{\mathbf{q}}(s), \quad (20)$$

$$b'(s) = 2a(s), \quad (21)$$

$$|\boldsymbol{\tau}(s)| \leq \boldsymbol{\mu}(s), \quad (22)$$

$$0 \leq \boldsymbol{\gamma}'(s)^2 b(s) \leq \boldsymbol{\psi}(s)^2, \quad (23)$$

$$|\ddot{\mathbf{q}}(s)| \leq \boldsymbol{\alpha}(s), \quad (24)$$

$$b(0) = 0, b(s_f) = 0, \quad (25)$$

where the squares of the two vectors $\boldsymbol{\gamma}'(s)$ and $\boldsymbol{\psi}(s)$ in (23) are to be intended component-wise. Problem 2 is convex since the objective function (18) is convex and the constraints (19)-(25) are linear.

The following proposition (that will be proved in the appendix) shows that Problem 2 admits a solution.

Proposition 1. *Problem 2 admits an optimal solution b^* , and moreover,*

$$\int_0^{s_f} b^*(s)^{-1/2} ds \leq U < \infty,$$

where U is a constant depending on problem data.

We do not directly solve Problem 2, but find an approximated solution based on a finite dimensional approximation. Namely, consider the following problem, obtained by uniformly sampling the interval $[0, s_f]$ in n points s_1, s_2, \dots, s_n from $s_1 = 0$ to $s_n = s_f$:

Problem 3.

$$\min_{\tau, a, b} 2h \sum_{i=1}^{n-1} \left(\frac{1}{b_i^{1/2} + b_{i+1}^{1/2}} \right). \quad (26)$$

$$\text{subject to } (i = 1, \dots, n-1) \quad (27)$$

$$\mathbf{d}_i a_i + \mathbf{c}_i b_i + \mathbf{g}_i = \boldsymbol{\tau}_i, \quad (28)$$

$$\boldsymbol{\gamma}'_i a_i + \boldsymbol{\gamma}''_i b_i = \ddot{\mathbf{q}}_i, \quad (29)$$

$$b_{i+1} - b_i = 2a_i h, \quad (30)$$

$$|\boldsymbol{\tau}_i| \leq \boldsymbol{\mu}_i, \quad (31)$$

$$|\ddot{\mathbf{q}}_i| \leq \boldsymbol{\alpha}_i \quad (32)$$

$$0 \leq [\boldsymbol{\gamma}'_i]^2 b_i \leq \boldsymbol{\psi}_i^2, \quad (33)$$

$$b_1 = 0, b_n = 0. \quad (34)$$

$$\mathbf{b} \in \mathbb{R}^n \quad \mathbf{a} \in \mathbb{R}^{n-1}, \boldsymbol{\tau}_i \in \mathbb{R}^p, \quad (35)$$

where $h = \frac{s_n}{n-1}$, $\boldsymbol{\alpha}_i = \boldsymbol{\alpha}(s_i)$, $\boldsymbol{\psi}_i = \boldsymbol{\psi}(s_i)$, $\boldsymbol{\mu}_i = \boldsymbol{\mu}(s_i)$, $\boldsymbol{\gamma}'_i = \boldsymbol{\gamma}'(s_i)$, $\boldsymbol{\gamma}''_i = \boldsymbol{\gamma}''(s_i)$, $\mathbf{d}_i = D(\boldsymbol{\gamma}_i)\boldsymbol{\gamma}'_i$, $\mathbf{c}_i = D(\boldsymbol{\gamma}_i)\boldsymbol{\gamma}''_i + C(\boldsymbol{\gamma}_i, \boldsymbol{\gamma}'_i)\boldsymbol{\gamma}'_i$, and $\mathbf{g}_i = \mathbf{g}(\boldsymbol{\gamma}_i)$, with $i = 1, \dots, n$.

Thank to constraints (28)-(30), it is possible to eliminate variables τ_i and a_i and use only b_i , with $i = 1, \dots, n$, as decision variables. The feasible set of Problem 3 is a non-empty set since $\mathbf{b} = 0$ is a feasible solution (in fact, it also has a nonempty interior).

Since Problem 3 is convex, we can easily find a solution with an interior point method (see [27]).

After solving Problem 3, it is possible to find an approximated solution of Problem 2. Indeed, by quadratic interpolation, we associate to a vector $\mathbf{b} \in \mathbb{R}^n$, solution of Problem 3, a continuously differentiable function $\mathcal{I}_{\mathbf{b}} : [0, s_f] \rightarrow \mathbb{R}$ such that the following relations hold for $i = 1, \dots, n-1$,

$$\begin{aligned}\mathcal{I}_{\mathbf{b}}(0) &= b_1, \quad \mathcal{I}_{\mathbf{b}}(s_f) = b_n, \\ \mathcal{I}_{\mathbf{b}}((i-1/2)h) &= \frac{b_i + b_{i+1}}{2}, \quad i = 1, \dots, n-1, \\ \mathcal{I}'_{\mathbf{b}}((i-1/2)h) &= \frac{b_{i+1} - b_i}{h}, \quad i = 1, \dots, n-1.\end{aligned}\tag{36}$$

Namely, $\mathcal{I}_{\mathbf{b}}$ interpolates b_1 and b_n at 0 and s_f , respectively, and the average values of consecutive entries of \mathbf{b} at the midpoint of the discretization intervals. Moreover, the derivative of $\mathcal{I}_{\mathbf{b}}$ at the midpoints of the discretization intervals corresponds to the finite differences of \mathbf{b} .

We define the class of quadratic splines \mathcal{P} as the subset of $\mathcal{C}^1([0, s_f], \mathbb{R})$, such that, for $i = 1, \dots, n-1$, $p|_{[h(i-\frac{1}{2}), h(i+\frac{1}{2})]}$ is a quadratic polynomial. For $i = 2, \dots, n-1$, let $x_i, y_i, z_i \in \mathbb{R}$ be such that:

$$p|_{[h(i-\frac{1}{2}), h(i+\frac{1}{2})]}(t) = x_i + y_i(t - hi) + z_i(t - hi)^2,$$

and let $x_1, y_1, z_1, x_n, y_n, z_n$ be such that

$$p|_{[0, h/2]}(t) = x_1 + y_1t + z_1t^2$$

and

$$p|_{[h(n-1/2), hn]}(t) = x_n + y_n(t - hn) + z_n(t - hn)^2.$$

For ease of notation, set, for $i = 1, \dots, n-1$,

$$\begin{aligned}b_{i-1/2} &= \frac{b_{i-1} + b_i}{2}, & b_{i+1/2} &= \frac{b_{i+1} + b_i}{2} \\ \delta_{i+1/2} &= \frac{b_{i+1} - b_i}{h}, & \delta_{i-1/2} &= \frac{b_i - b_{i-1}}{h}.\end{aligned}$$

The following proposition, whose proof is presented in appendix, defines the interpolating quadratic spline fulfilling (36).

Proposition 2. *For any $\mathbf{b} \in \mathbb{R}^n$, there exists a unique element $p \in \mathcal{P}$ such that the following interpolation conditions hold*

$$\begin{aligned}p(h(i + \tfrac{1}{2})) &= b_{i+1/2}, & i &= 1, \dots, n-1, \\ p'(h(i + \tfrac{1}{2})) &= \delta_{i+1/2}, & i &= 1, \dots, n-1, \\ p(0) &= b_1, & p(s_f) &= b_n.\end{aligned}\tag{37}$$

Note that p is continuously differentiable and that (36) holds. Such element will be denoted by $\mathcal{I}_{\mathbf{b}}$.

Note that by Proposition 2, there exists a unique function $b = \mathcal{I}_b$ that interpolates the solution of Problem 3. Then a and τ are computed from b by using relations (17) and (19), namely we set ($\forall s \in [0, s_f]$)

$$a(s) = \frac{b'(s)}{2},$$

$$\tau(s) = \mathbf{d}(s)a(s) + \mathbf{c}(s)b(s) + \mathbf{g}(s).$$

Functions b , a and τ are approximate solutions of Problem 2. Indeed, (26) and (30) are approximations of (18) and (21), moreover, functions b , a and τ satisfy, by construction, constraints (19)-(25) for $s \in \{s_1, \dots, s_n\}$ and by continuity, (19)-(25) are also approximately satisfied for $s \in [0, s_f]$. By increasing the number of samples n , the solutions of Problem 3 become better approximations of the solutions of Problem 2. It is reasonable to suppose that, as n approaches to $+\infty$, the solutions of Problem 3 converge to the solutions of Problem 2. Anyway this convergence property is not proved in this paper being outside its scope. It can be proved on the lines of [2], that presents a convergence result for a related speed planning problem for an autonomous vehicle.

3 Solution algorithms and complexity issues for the generalized problem

In this section we present an optimal time complexity algorithm that solves a specific class of optimization problems. In the subsequent section we will show that Problem 2 can be approximated by a finite dimensional problem that belongs to this class.

3.1 Exact algorithm for the solution of some special structured problems

The problems under consideration have the form

$$\begin{aligned} \min \quad & g(v_1, \dots, v_n) \\ & v_i \leq f_j^i(v_{i+1}) \quad i = 1, \dots, n-1, \\ & \quad \quad \quad j = 1, \dots, r_i \\ & v_{i+1} \leq b_k^i(v_i) \quad i = 1, \dots, n-1, \\ & \quad \quad \quad k = 1, \dots, t_i, \\ & 0 \leq v_i \leq u_i \quad i = 1, \dots, n, \end{aligned} \tag{38}$$

where we make the following assumptions.

Assumption 3. *We assume:*

- g monotonic non increasing;
- f_j^i , concave, increasing and $f_j^i(0) > 0$,
 $i = 1, \dots, n-1, \quad j = 1, \dots, r_i$;
- b_k^i , concave, increasing and $b_k^i(0) > 0$,
 $i = 1, \dots, n-1, \quad k = 1, \dots, t_i$.

The constraints in (38) can be rewritten in compact form as follows:

$$\begin{aligned} v_i &\leq \min\{B_i(v_{i+1}), u_i\} & i = 1, \dots, n-1, \\ v_{i+1} &\leq \min\{F_i(v_i), u_{i+1}\} & i = 1, \dots, n-1, \end{aligned}$$

where:

$$\begin{aligned} B_i(v_{i+1}) &= \min_{j=1, \dots, r_i} f_j^i(v_{i+1}), \\ F_i(v_i) &= \min_{k=1, \dots, t_i} b_k^i(v_i). \end{aligned}$$

Note that F_i and B_i are both concave and increasing over \mathbb{R}_+ , since they are the minimum of a finite number of functions with the same properties. We prove that the same holds for $F_i \circ B_i$.

Proposition 3. $F_i \circ B_i$ is increasing and concave over \mathbb{R}_+ .

Proof. The fact that $F_i \circ B_i$ is increasing follows immediately from the increasingness of F_i and B_i . For what concerns concavity, $\forall x, y \geq 0, \lambda \in [0, 1]$:

$$\begin{aligned} F_i \circ B_i(\lambda x + (1 - \lambda)y) &= F_i(B_i(\lambda x + (1 - \lambda)y)) \\ &\geq F_i(\lambda B_i(x) + (1 - \lambda)B_i(y)) \geq \lambda F_i \circ B_i(x) + (1 - \lambda)F_i \circ B_i(y), \end{aligned}$$

where the first inequality is a consequence of the concavity of B_i and the fact that F_i is increasing, while the second inequality comes from concavity of F_i . \square

It immediately follows that:

$$F_i \circ B_i(x) - x \text{ concave, } F_i \circ B_i(0) > 0. \quad (39)$$

Then, there exists at most one point $\bar{v}_{i+1} > 0$ such that $F_i \circ B_i(\bar{v}_{i+1}) - \bar{v}_{i+1} = 0$. Similarly, there exists at most one point $\bar{v}_i > 0$ such that $B_i \circ F_i(\bar{v}_i) - \bar{v}_i = 0$. Note that \bar{v}_i, \bar{v}_{i+1} are the positive fixed points of $B_i \circ F_i$ and $F_i \circ B_i$, respectively. Alternatively, $(\bar{v}_i, \bar{v}_{i+1})$ is also the optimal solution of the following two-dimensional convex problem:

$$\begin{aligned} \max \quad & v_i + v_{i+1} \\ \text{s.t.} \quad & v_i \leq f_j^i(v_{i+1}) \quad j = 1, \dots, r_i \\ & v_{i+1} \leq b_k^i(v_i) \quad k = 1, \dots, t_i. \end{aligned}$$

The following result holds.

Proposition 4. Under Assumption 3, the optimal solution of (38) is the component-wise maximum of its feasible region, i.e., if we denote by X the feasible region, it is the point $\mathbf{v}^* \in X$ such that $\mathbf{v} \leq \mathbf{v}^*$ for all $\mathbf{v} \in X$.

Proof. See [3, 16]. \square

We consider Algorithm 1 for the solution of problem (38). The algorithm is correct, as stated in the following proposition.

Proposition 5. Algorithm 1 returns the optimal solution \mathbf{v}^* of problem (38).

```

Data:  $\mathbf{u} \in \mathbb{R}_+^n$ ;
1 Set  $\bar{\mathbf{u}} = \mathbf{u}$ ;
2 /* Forward phase */
3 ;
4 foreach  $i \in \{1, \dots, n-1\}$  do
5   Compute the nonnegative fixed points  $\bar{v}_i$  and  $\bar{v}_{i+1}$  for  $B_i \circ F_i$  and  $F_i \circ B_i$ ,
   respectively (if they do not exist, set  $\bar{v}_i = +\infty$ ,  $\bar{v}_{i+1} = +\infty$ );
6   Set  $\bar{u}_i = \min\{\bar{u}_i, B_i(\bar{u}_{i+1}), \bar{v}_i\}$ ;
7   Set  $\bar{u}_{i+1} = \min\{\bar{u}_{i+1}, F_i(\bar{u}_i), \bar{v}_{i+1}\}$ ;
8 end
9 /* Backward phase */
10 ;
11 foreach  $i \in \{n-1, \dots, 1\}$  do
12   Set  $\bar{u}_i = \min\{B_i(\bar{u}_{i+1}), \bar{u}_i\}$ ;
13 end

```

Algorithm 1: Forward-Backward algorithm for the solution of the problem.

Proof. We first remark that at each iteration $\bar{\mathbf{u}} \geq \mathbf{v}^*$ holds. If a fixed point \bar{v}_{i+1} for $F_i \circ B_i$ exists, then after the backward propagation, $\bar{u}_{i+1} \leq \bar{v}_{i+1}$, and $\bar{u}_i = \min\{\bar{u}_i^{old}, B_i(\bar{u}_{i+1})\}$, where \bar{u}_i^{old} denotes the upper bound for v_i after the forward phase. We show that

$$F_i(\bar{u}_i) = \min\{F_i(\bar{u}_i^{old}), F_i \circ B_i(\bar{u}_{i+1})\} \geq \bar{u}_{i+1}. \quad (40)$$

If this is true for all i , then the point $\bar{\mathbf{u}}$ at the end of the backward phase is a feasible solution of (38). Indeed, by definition of \bar{u}_i in the backward phase, $\forall i$

$$\bar{u}_i \leq B_i(\bar{u}_{i+1}),$$

while by (40), $\forall i$

$$\bar{u}_{i+1} \leq F_i(\bar{u}_i),$$

so that $\bar{\mathbf{u}}$ is feasible for (38). Since $\bar{\mathbf{u}} \geq \mathbf{v}^*$ holds and g is monotone non increasing, we have that $\bar{\mathbf{u}}$ is the optimal solution of (38). We only need to prove that (40) is true. Note that \bar{u}_i^{old} is the result of the first forward propagation, so that $F_i(\bar{u}_i^{old}) \geq \bar{u}_{i+1}^{old} \geq \bar{u}_{i+1}$. Thus, we need to prove that $F_i \circ B_i(\bar{u}_{i+1}) \geq \bar{u}_{i+1}$ with $\bar{u}_{i+1} \leq \bar{v}_{i+1}$. In view of (39), if the fixed point \bar{v}_{i+1} for $F_i \circ B_i$ exists, it is the unique nonnegative root of $F_i \circ B_i(x) - x$ and

$$F_i \circ B_i(x) - x > 0 \quad \forall x \leq \bar{v}_{i+1},$$

from which the result is proved. Otherwise, if no fixed point exists,

$$F_i \circ B_i(x) - x > 0 \quad \forall x \in \mathbb{R}_+,$$

from which the result is still proved. □

Under a given condition, Algorithm 1 can be further simplified.

Remark 1. If F_i and B_i , $i = 1, \dots, n$, fulfill the so called superiority condition, i.e.

$$F_i(x), B_i(x) > x \quad \forall x \in \mathbb{R}_+,$$

then $\bar{v}_i, \bar{v}_{i+1} = +\infty$ and the forward phase can be reduced to

$$\bar{u}_{i+1} = \min\{\bar{u}_{i+1}, F_i(\bar{u}_i)\}.$$

3.2 Solving the subproblems in the forward phase and complexity results

We first remark that

$$\bar{u}_i = \min\{\bar{u}_i, B_i(\bar{u}_{i+1}), \bar{v}_i\},$$

$$\bar{u}_{i+1} = \min\{\bar{u}_{i+1}, F_i(\bar{u}_i), \bar{v}_{i+1}\},$$

defined in the forward phase of Algorithm 1 are the solution of the two-dimensional convex optimization problem

$$\begin{aligned} \max \quad & v_i + v_{i+1} \\ & v_i \leq f_j^i(v_{i+1}) \quad j = 1, \dots, r_i \\ & v_{i+1} \leq b_k^i(v_i) \quad k = 1, \dots, t_i \\ & 0 \leq v_i \leq f_{r_i+1}^i(v_{i+1}) \equiv \bar{u}_i \\ & 0 \leq v_{i+1} \leq b_{t_i+1}^i(v_i) \equiv \bar{u}_{i+1}. \end{aligned} \tag{41}$$

Alternatively, \bar{u}_i, \bar{u}_{i+1} can also be detected as fixed points of $B_i^{\bar{u}} \circ F_i^{\bar{u}}$ and $F_i^{\bar{u}} \circ B_i^{\bar{u}}$, respectively, where

$$F_i^{\bar{u}}(x) = \min\{\bar{u}_i, F_i(x)\},$$

$$B_i^{\bar{u}}(x) = \min\{\bar{u}_{i+1}, B_i(x)\}.$$

Although any convex optimization or any fixed point solver could be exploited for detecting these values, we propose the simple Algorithm 2, which turns out to be quite effective in practice. We denote by

$$[F_i]^{-1}(x) = \max_{j=1, \dots, r_i} \{[f_j^i]^{-1}(x)\}.$$

Note that f_j^i increasing and concave implies that $[f_j^i]^{-1}$ is increasing and convex and, consequently, $[F_i]^{-1}$ is increasing and convex. We illustrate how the algorithm works through an

```

1 Let  $\bar{x}_1 = \bar{u}_i$ ;
2 Set  $\bar{y} = -\infty, \bar{z} = +\infty, h = 1$ ;
3 while  $\bar{y} < \bar{z}$  do
4   Set  $\bar{y} = B_i^{\bar{u}}(\bar{x}_h)$  and  $\bar{k} \in \{1, \dots, t_i + 1\} : b_{\bar{k}}^i(\bar{x}_h) = \bar{y}$ ;
5   Set  $\bar{z} = [F_i]^{-1}(\bar{x}_h)$  and  $\bar{j} \in \{1, \dots, r_i\} : [f_{\bar{j}}^i]^{-1}(\bar{x}_h) = \bar{z}$ ;
6   Let  $\bar{x}_{h+1}$  be the solution of the one-dimensional equation  $f_{\bar{j}}^i(b_{\bar{k}}^i(x)) = x$ ;
7   Set  $h = h + 1$ ;
8 end
9 return  $(\bar{u}_i, \bar{u}_{i+1}) = (\bar{x}_h, \bar{y})$ ;
```

Algorithm 2: Algorithm for the computation of the new values \bar{u}_i and \bar{u}_{i+1} .

example.

Example 1. Let

$$b_1^i(x) = \frac{3}{2}x + 2, \quad b_2^i(x) = x + 3,$$

$$b_3^i(x) = \frac{1}{2}x + 5, \quad b_4^i(x) = 8.$$

and

$$[f_1^i]^{-1}(x) = x - 1, \quad [f_2^i]^{-1}(x) = \frac{9}{2}x - 8,$$

$$[f_3^i]^{-1}(x) = 5x - 10.$$

Moreover, let $u_i = u_{i+1} = 8$. Then, we initially set $\bar{x}_1 = 8$.

In the first iteration we have

$$\bar{y} = B_i^{\bar{u}}(\bar{x}_1) = \min_{k=1,\dots,4} \{b_k^i(\bar{x}_1)\} = \min\{14, 11, 9, 8\} = 8,$$

with $\bar{k} = 4$, and

$$\bar{z} = [F_i]^{-1}(\bar{x}_1) = \max_{j=1,\dots,3} \{[f_j^i]^{-1}(\bar{x}_1)\} = \max\{7, 28, 30\} = 30,$$

with $\bar{j} = 3$. Then, \bar{x}_2 is the solution of the equation $8 = 5x - 10$, i.e., $\bar{x}_2 = \frac{18}{5}$ (See also Figure 1). In the second iteration we have

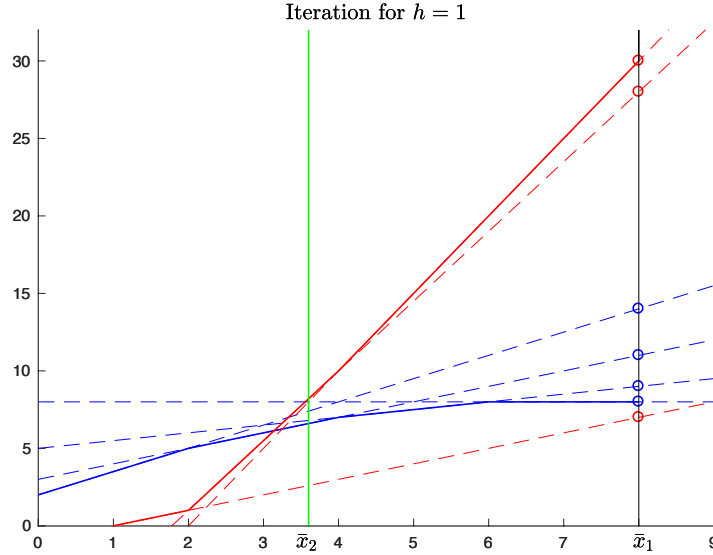


Figure 1: The first step of Algorithm 2. The red lines represent the linear function $[f_j^i]^{-1}$ while the blue ones are the functions $b_{\bar{k}i}$. The green line represents the solution of the one dimensional equation $f_j^i(b_{\bar{k}i}(x)) = x$.

$$\bar{y} = B_i^{\bar{u}}(\bar{x}_2) = \min_{k=1,\dots,4} \{b_k^i(\bar{x}_2)\} = \min \left\{ \frac{37}{5}, \frac{33}{5}, \frac{34}{5}, 8 \right\} = \frac{33}{5},$$

with $\bar{k} = 2$, and

$$\bar{z} = [F_i]^{-1}(\bar{x}_2) = \max_{j=1,\dots,3} \{[f_j^i]^{-1}(\bar{x}_2)\} = \max \left\{ \frac{13}{5}, \frac{41}{5}, 8 \right\} = \frac{41}{5},$$

with $\bar{j} = 2$. Then, \bar{x}_3 is the solution of the equation $x + 3 = \frac{9}{2}x - 8$, i.e., $\bar{x}_3 = \frac{22}{7}$ (See also Figure 2).

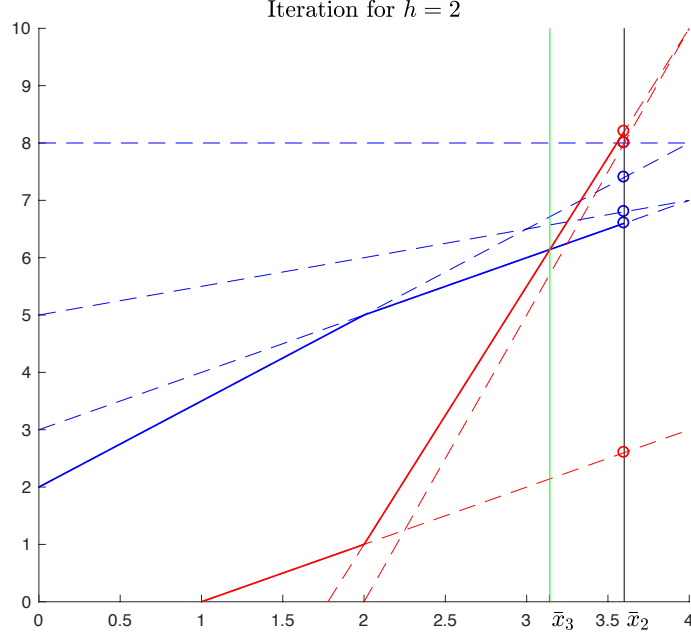


Figure 2: The second step of Algorithm 2.

In the third iteration we have

$$\bar{y} = B_i^{\bar{u}}(\bar{x}_3) = \min_{k=1,\dots,4} \{b_k^i(\bar{x}_3)\} = \min \left\{ \frac{47}{7}, \frac{43}{7}, \frac{46}{7}, 8 \right\} = \frac{43}{7},$$

with $\bar{k} = 2$, and

$$\bar{z} = [F_i]^{-1}(\bar{x}_3) = \max_{j=1,\dots,3} \{[f_j^i]^{-1}(\bar{x}_3)\} = \max \left\{ \frac{15}{7}, \frac{43}{7}, \frac{40}{7} \right\} = \frac{43}{7},$$

with $\bar{j} = 2$. Then, $\bar{x}_4 = \bar{x}_3$ and since $\bar{y} = \bar{z}$ the algorithm stops and returns the optimal solution $(\frac{22}{7}, \frac{43}{7})$ (See also Figure 3).

If we denote by C_b the time needed to evaluate one function b_k^i , by C_f the time needed to evaluate one function $[f_j^i]^{-1}$, and by C_{eq} the time needed to solve a one-dimensional equation $f_j^i(b_k^i(x)) = x$, we can state the complexity of Algorithm 2. Before we need to prove one lemma.

Lemma 1. *The sequence $\{\bar{x}_h\}$ is strictly decreasing.*

Proof. If the algorithm does not stop, then $\bar{y} < \bar{z}$, or, equivalently

$$b_{\bar{k}}^i(\bar{x}_h) - [f_{\bar{j}}^i]^{-1}(\bar{x}_h) < 0.$$

Since $[f_{\bar{j}}^i]^{-1}$ is convex, $b_{\bar{k}}^i(x) - [f_{\bar{j}}^i]^{-1}(x)$ is concave. Moreover, $b_{\bar{k}}^i(0) - [f_{\bar{j}}^i]^{-1}(0) > 0$. Then, there exists a unique value $x \in (0, \bar{x}_h)$ such that

$$b_{\bar{k}}^i(x) - [f_{\bar{j}}^i]^{-1}(x) = 0.$$

Such value, lower than \bar{x}_h , is also the solution \bar{x}_{h+1} of the one-dimensional equation $f_{\bar{j}}^i(b_{\bar{k}}^i(x)) = x$. \square

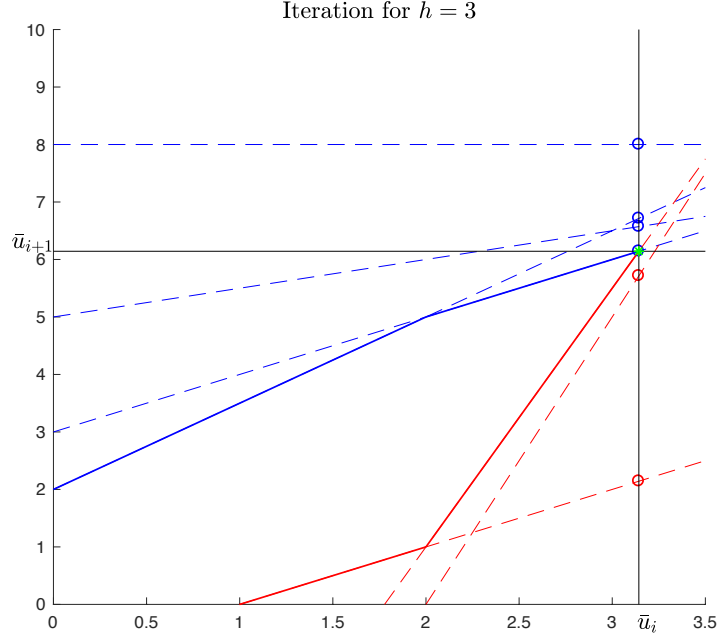


Figure 3: The last step of Algorithm 2. The green marker represents value $(u_i, u_{i+1}) = (\bar{x}_h, \bar{y})$ returned.

Now we are ready to prove the complexity result.

Proposition 6. *Algorithm 2 has complexity $O(r_i t_i (t_i C_b + r_i C_f + C_{eq}))$.*

Proof. In view of Lemma 1 the sequence $\{\bar{x}_h\}$ is decreasing, which means that an equation $f_j^i(b_k^i(x)) = x$, $j = 1, \dots, r_i$, $k = 1, \dots, t_i + 1$, is solved at most once. Thus, the number of iterations is at most $(t_i + 1)r_i$. At each iteration we need to evaluate $B_i^{\bar{u}}$ $((t_i + 1)C_b$ operations), evaluate $[F_i]^{-1}$ $(r_i C_f$ operations), and solve a one-dimensional equation (C_{eq} operations). \square

Algorithm 2 and the related complexity result can be improved when the functions b_k^i and f_j^i are linear ones. The linear case is particularly relevant in our context since a suitable discretization of Problem 2 will turn out to fall into this case, as we will see in Section 4. Algorithm 3 is a variant of Algorithm 2 for the linear case. In the initialization phase of Algorithm 3 the slopes m_k , $k = 1, \dots, t_i + 1$, of the linear functions b_k^i are ordered in a decreasing way, i.e.,

$$m_k > m_{k+1}, \quad k = 1, \dots, t_i,$$

while the slopes η_j , $j = 1, \dots, r_i$, of the linear functions $[f_j^i]^{-1}$ are ordered in a decreasing way, i.e.,

$$\eta_j < \eta_{j+1}, \quad j = 1, \dots, r_i - 1.$$

Note that, in case of two linear functions with the same slope, one of the two can be eliminated since it gives rise to a redundant constraint. The pointer ξ is updated in such a way that at each iteration it identifies the index \bar{k} such that $\bar{y} = B_i^{\bar{u}}(\bar{x}_h) = b_{\bar{k}}^i(\bar{x}_h)$, without the need of computing the value of *all* the functions b_k^i (as, instead, required in Algorithm 2) and, thus, saving the $O(t_i)$ time required by this computation. Similarly, the pointer ϕ is updated in such a way that at each iteration it identifies the index \bar{j} such that $\bar{z} = [F_i]^{-1}(\bar{x}_h) = [f_{\bar{j}}^i]^{-1}(\bar{x}_h)$. We illustrate the algorithm on the previous example.

```

1 Order the slopes of the linear functions  $b_k^i$ ,  $k = 1, \dots, t_i + 1$ , in a decreasing way;
2 Order the slopes of the linear functions  $[f_j^i]^{-1}$ ,  $j = 1, \dots, r_i$ , in an increasing way;
3 Set  $\xi = t_i + 1$  and  $\phi = r_i$ ;
4 Let  $\bar{x}_1 = \bar{u}_i$ ;
5 Set  $\bar{y} = -\infty$ ,  $\bar{z} = +\infty$ ,  $h = 1$ ;
6 while  $\bar{y} < \bar{z}$  do
7   while  $\xi > 1$  and  $b_{\xi-1}^i(\bar{x}_h) < b_\xi^i(\bar{x}_h)$  do
8     | Set  $\xi = \xi - 1$ ;
9   end
10  Set  $\bar{k} = \xi$  and  $\bar{y} = b_{\bar{k}}^i(\bar{x}_h)$ ;
11  while  $\phi > 1$  and  $[f_{\phi-1}^i]^{-1}(\bar{x}_h) > [f_\phi^i]^{-1}(\bar{x}_h)$  do
12    | Set  $\phi = \phi - 1$ ;
13  end
14  Set  $\bar{j} = \phi$  and  $\bar{z} = [f_{\bar{j}}^i]^{-1}(\bar{x}_h)$ ;
15  Let  $\bar{x}_{h+1}$  be the solution of the one-dimensional equation  $f_{\bar{j}}^i(b_{\bar{k}}^i(x)) = x$ ;
16  Set  $h = h + 1$ ;
17 end
18 return  $(\bar{u}_i, \bar{u}_{i+1}) = (\bar{x}_h, \bar{y})$ ;

```

Algorithm 3: Algorithm for the computation of the new values \bar{u}_i and \bar{u}_{i+1} in the linear case.

Example 2. The slopes of the functions b_k^i are already ordered in a decreasing way, while those of the functions $[f_j^i]^{-1}$ are already ordered in an increasing way.

In the first iteration we immediately exit the first inner **While** cycle since $b_4^i(\bar{x}_1) < b_3^i(\bar{x}_1)$, so that at the end of the cycle we set $\bar{k} = \xi = 4$. We also immediately exit the second inner **While** cycle since $[f_3^i]^{-1}(\bar{x}_1) > [f_2^i]^{-1}(\bar{x}_1)$, so that at the end of the cycle we set $\bar{j} = \phi = 3$. In the second iteration the first inner **While** cycle is repeated twice since

$$b_4^i(\bar{x}_2) > b_3^i(\bar{x}_2) > b_2^i(\bar{x}_2) < b_1^i(\bar{x}_2),$$

so that at the end of the cycle we set $\bar{k} = \xi = 2$. The second inner **While** cycle is repeated once since

$$[f_3^i]^{-1}(\bar{x}_1) < [f_2^i]^{-1}(\bar{x}_2) > [f_1^i]^{-1}(\bar{x}_2),$$

so that at the end of the cycle we set $\bar{j} = \phi = 2$.

In the third iteration we immediately exit the first inner **While** cycle since $b_2^i(\bar{x}_1) < b_1^i(\bar{x}_3)$, so that at the end of the cycle we set $\bar{k} = \xi = 2$. We also immediately exit the second inner **While** cycle since $[f_2^i]^{-1}(\bar{x}_3) > [f_1^i]^{-1}(\bar{x}_3)$, so that at the end of the cycle we set $\bar{j} = \phi = 2$.

The following proposition establishes the complexity of Algorithm 3.

Proposition 7. Algorithm 3 has complexity $O(r_i \log(r_i) + t_i \log(t_i))$.

Proof. We first remark that the initial orderings of the slopes already require the computing time $O(r_i \log(r_i) + t_i \log(t_i))$. Next, we remark that in the linear case C_b, C_f and C_{eq} are $O(1)$ operations. In particular, the one-dimensional equation is a linear one. Moreover, we notice that B_i^u is a concave piecewise linear function, while $[F_i]^{-1}$ is a convex piecewise

linear function. Since in view of Lemma 1 the sequence $\{\bar{x}_h\}$ is decreasing, the corresponding sequence of slopes of the function $B_i^{\bar{u}}$ at points \bar{x}_h is not decreasing, while the sequence of slopes of the function $[F_i]^{-1}$ is not increasing, and at each iteration at least one slope must change (otherwise we would solve the same linear equation and \bar{x}_h would not change). Then, the number of different slope values and, thus, the number of iterations, can not be larger than $t_i + r_i + 1$. Moreover, by updating the two pointers ξ and ϕ , the overall number of evaluations of the functions b_k^i and $[f_j^i]^{-1}$, needed to compute the different values \bar{y} and \bar{z} in the outer **While** cycle can not be larger than $O(t_i + r_i)$. Consequently, the computing time of the outer **While** cycle is $O(t_i + r_i)$ and the complexity of the algorithm is determined by the initial orderings of the slopes. \square

While in practice we employed Algorithm 3 to compute \bar{u}_i, \bar{u}_{i+1} , in the linear case we could also solve the linear subproblem (41). This can be done in linear time $O(t_i + r_i)$ with respect to the number of constraints, e.g., by Megiddo's algorithm (see [12]). Thus, we can state the following complexity result for Problem (38) in the linear case.

Theorem 1. *If $f_j^i, b_k^i, i = 1, \dots, n, j = 1, \dots, r_i$, and $k = 1, \dots, t_i$, are linear functions, then Problem (38) can be solved in time $O(\sum_{i=1}^n (t_i + r_i))$ by Algorithm 1, if \bar{u}_i, \bar{u}_{i+1} are computed by Megiddo's algorithm. Such complexity is optimal.*

Proof. The complexity result immediately follows by the observation that the most time consuming part of Algorithm 1 is the forward one with the computation of \bar{u}_i, \bar{u}_{i+1} . Indeed, the backward part is run in $O(\sum_{i=1}^n t_i)$ time (at each iteration we only need to evaluate B_i). The fact that such complexity is optimal follows from the observation that $O(\sum_{i=1}^n (t_i + r_i))$ is also the size of the input values for the problem. \square

4 Discretization of the speed-planning problem

Problem 3 does not belong to the class defined in (38). In this section, we show that a small variation of Problem 2, followed by discretization, allows obtaining a problem that belongs to class (38).

To this end, consider the following family of problems, depending on the positive real parameter h .

Problem 4.

$$\min_{a, \tau \in C^0, b \in C^1} \int_0^{s_f} b(s)^{-1/2} ds, \quad (42)$$

subject to $(\forall s \in [0, s_f], j = 1, \dots, p)$

$$b(s + \lambda_j(s)) = \hat{b}_j(s) \quad (43)$$

$$b(s + \eta_j(s)) = \bar{b}_j(s) \quad (44)$$

$$d_j(s)a(s) + c_j(s)\hat{b}_j(s) + g(s) = \tau_j(s), \quad (45)$$

$$\gamma'_j(s)a(s) + \gamma''_j(s)\bar{b}_j(s) = \ddot{q}_j(s), \quad (46)$$

$$b'(s) = 2a(s), \quad (47)$$

$$|\ddot{\mathbf{q}}(s)| \leq \boldsymbol{\alpha}(s), \quad (48)$$

$$0 \leq \gamma'(s)^2 b(s) \leq \psi(s)^2, \quad (49)$$

$$|\tau(s)| \leq \boldsymbol{\mu}(s), \quad (50)$$

$$b(0) = 0, b(s_f) = 0, \quad (51)$$

$$(52)$$

where functions λ_j and η_j are defined as follows $(\forall s \in [0, s_f]$ and $j = 1, \dots, p)$:

$$\lambda_j(s) = \begin{cases} h, & d_j(s)c_j(s) \geq 0 \\ 0, & d_j(s)c_j(s) \leq 0, \end{cases} \quad (53)$$

$$\eta_j(s) = \begin{cases} h, & \gamma'_j(s)\gamma''_j(s) \geq 0 \\ 0, & \gamma'_j(s)\gamma''_j(s) \leq 0. \end{cases} \quad (54)$$

Note that, for $h = 0$, Problem 4 becomes Problem 2. Further, for every $h > 0$, Problem 4 has an optimal solution (this can be proved with the same arguments used for Proposition 1). Let b_h^* be the solution of Problem 4 as a function of h . Note that, by (46) and (48), $\forall h > 0, \forall s \in [0, s_f], |b'(s)| \leq L = 2\sqrt{p}(\|\boldsymbol{\alpha}\| + p\|\boldsymbol{\gamma}''\|\|\boldsymbol{\psi}\|^2)$ so that b_h^* is Lipschitz with constant L , independent of h . Thus, Ascoli-Arzelà Theorem implies that from any succession of solutions $b_{h_i}^*$, with $\lim_{i \rightarrow \infty} h_i = 0$ we can extract a convergent subsequence that converges to a solution of Problem 2.

Discretizing Problem 4 with step h , we obtain the following problem.

Problem 5.

$$\min_{\mathbf{a}, \mathbf{b}, \boldsymbol{\tau}} 2h \sum_{i=1}^{n-1} \left(\frac{1}{b_i^{1/2} + b_{i+1}^{1/2}} \right), \quad (55)$$

$$\text{subject to } (i = 1, \dots, n-1) \quad (56)$$

$$\lambda_i b_{i+1} + (1 - \lambda_i) b_i = \hat{\mathbf{b}}_i, \quad (57)$$

$$\eta_i b_{i+1} + (1 - \eta_i) b_i = \bar{\mathbf{b}}_i, \quad (58)$$

$$\mathbf{d}_i a_i \mathbf{1} + \mathbf{c}_i \hat{\mathbf{b}}_i + \mathbf{g}_i = \boldsymbol{\tau}_i, \quad (59)$$

$$\gamma'_i a_i \mathbf{1} + \gamma''_i \bar{\mathbf{b}}_i = \ddot{\mathbf{q}}_i \quad (60)$$

$$b_{i+1} - b_i = 2a_i h, \quad (61)$$

$$|\boldsymbol{\tau}_i| \leq \boldsymbol{\mu}_i, \quad (62)$$

$$0 \leq \gamma_i'^2 b_i \leq \boldsymbol{\psi}_i^2, \quad (63)$$

$$|\ddot{\mathbf{q}}_i| \leq \boldsymbol{\alpha}_i, \quad (64)$$

$$b_1 = 0, b_n = 0. \quad (65)$$

$$\mathbf{b} \in \mathbb{R}^n \quad \mathbf{a} \in \mathbb{R}^{n-1}, \boldsymbol{\tau}_i \in \mathbb{R}^p. \quad (66)$$

Here, for $j = 1, \dots, p$, $i = 1, \dots, n$,

$$\lambda_{j,i} = \begin{cases} 1, & d_{j,i} c_{j,i} \geq 0 \\ 0, & d_{j,i} c_{j,i} < 0, \end{cases}$$

$$\eta_{j,i} = \begin{cases} 1, & \gamma'_{j,i} \gamma''_{j,i} \geq 0 \\ 0, & \gamma'_{j,i} \gamma''_{j,i} < 0. \end{cases}$$

The following proposition will be proved in the appendix.

Proposition 8. *Problem 5 belongs to problem class (38).*

4.1 Comparison with TOPP-RA algorithm ([19])

As already mentioned in the introduction, a very recent and interesting work, closely related to ours, is [19]. In that paper a backward-forward approach is proposed. In the backward phase a controllable set is computed for each discretization point. This is an interval that contains all possible states for which there exists at least a sequence of controls leading to the final assigned state. The computation of each interval requires the solution of two LP problems with two variables. Next, a forward phase is performed where a single LP with two variables is solved for each discretization point. The final result is a feasible solution which, however, is optimal under the assumption that no zero-inertia points are present. In the presence of zero-inertia points a solution is returned whose objective function value differs from the optimal one by a quantity proportional to the discretization step h . The overall number of two-dimensional LPs solved by this approach is $3n$, while in our approach we solve in total only n LPs. In [19] the LPs are solved by the simplex method while we proposed an alternative method which turns out to be more efficient. Indeed, our computational experiments will show that the computation times are reduced by at least an order of magnitude when using our alternative method. In [19] it is observed that the practical (say, average) complexity of

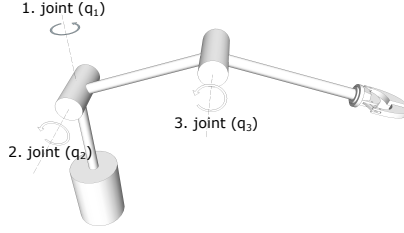


Figure 4: The 3-DoF manipulator with the three revolute joints ($\mathbf{q} = [q_1, q_2, q_3]^T$).

Table 1: Kinematic and dynamic parameters for the 3-DoF manipulator.

Link	$(I_{xi}, I_{yi}, I_{zi}) [kg \cdot m^2]$	$m_i [kg]$	$l_i [m]$	$r_i [m]$
1	(7.5, 7.5, 7.5)	1.5	0.2	0.08
2	(5.7, 5.7, 5.7)	1.2	0.3	0.12
3	(4.75, 4.75, 4.75)	1.0	0.325	0.13

the simplex method is linear with respect to the number of constraints. In fact, we observed that for two-dimensional LPs such complexity is not only the practical one but also the worst-case one. Finally, in our approach we deal with the presence of zero-inertia points through the addition of the displacements (53)-(54). Introducing these displacement, we are able to return an exact solution of the discretized problem.

5 Experimental results

In this section, we consider a motion planning problem for a 3-DoF manipulator and compare the computation time of the proposed solver to other methods existing in literature. We also show an experiment on the execution of a time-optimal velocity profile on a 6-DoF robotic manipulator.

5.1 Test case on a 3-DOF manipulator

We consider the robot presented in [15] (Chapter 4, example 4.3). This robot is a serial chain robot (see Figure 4), composed of 3 links connected with 3 revolute joints (the first link is connected with a fixed origin). Table 1 reports the robot parameters. Namely, for link i , $i = 1, \dots, 3$, l_i is the length, and r_i is the distance between the gravity center of the link and the joint that connects it to the previous link in the chain (see Figure 5). Parameters $I_{xi}, I_{yi}, I_{zi}, m_i$ are the diagonal components of the inertia matrix and the mass of link i .

We consider an instance of Problem 2, where the reference curve $\gamma : [0, 1] \rightarrow \mathbb{R}^3$ is defined as a cubic spline that interpolates the points shown in Table 2. The mass matrix \mathbf{D} , the Coriolis matrix \mathbf{C} and the external forces term \mathbf{g} that we consider are reported in [15] (Chapter 4, example 4.3).

The following kinematic and dynamic bounds are applied for the presented test case ($\forall s \in [0, 1]$)

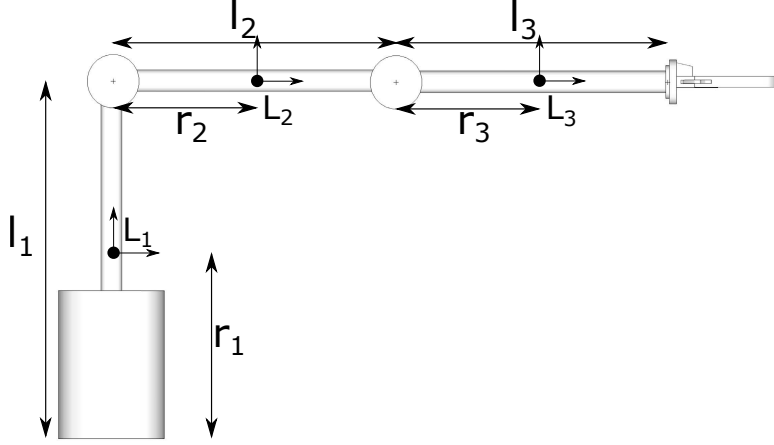


Figure 5: Kinematic and dynamic parameters for the 3-DoF manipulator. L_i indicates the coordinate frame attached to the gravity center of the link.

Table 2: Points interpolated in the configuration space.

s	γ_1	γ_2	γ_3
0	0	0	0
0.25	1.288	-0.2864	-0.2982
0.5	2.59	-0.03045	-0.5995
0.75	4.374	-0.04647	-0.582
1	5.334	-0.1657	-0.4504

$$\psi(s) = [2.0, 2.0, 2.0]^T$$

$$\alpha(s) = [1.5, 1.5, 1.5]^T$$

$$\mu(s) = [9, 9, 9]^T.$$

5.2 Computational time comparison

We find an approximated solution of Problem 2 by solving Problem 5 with four different methods.

1. a SOCP solver which solves the SOCP reformulation presented in Equation (74)-(86) of [27];
2. a LP solver which solves the LP reformulation presented in Equation (23) of [16];
3. Algorithm 1 using simplex method to solve the two-dimensional LP subproblems (41).
4. Algorithm 1 using Algorithm 3 to solve the two-dimensional LP subproblems (41).

In the first and second method we use Gurobi solver [8] while for the other methods we use a C++ implementation of Algorithm 1. We measure the performance on a 2.4 GHz Intel(R) Core(TM) i7-3630QM CPU.

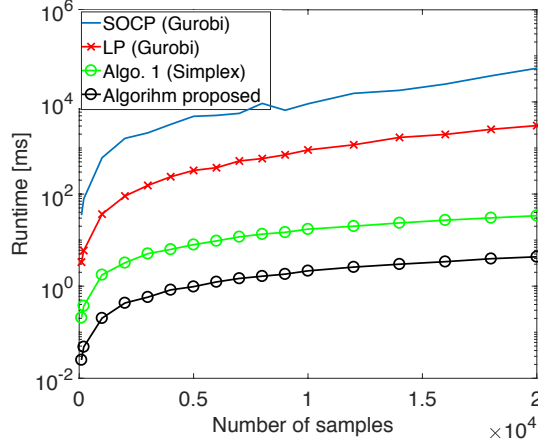


Figure 6: Computation times obtained using different approaches as a function of the number of variables.

The results presented in Figure 6 show that the Algorithm 1 with Algorithm 3 employed to solve the two-dimensional LP subproblems significantly outperforms the other methods (in particular, by more than four, two, and one of order of magnitude, respectively). We did not compute directly the solution with the TOPP-RA algorithm presented in [19], however, note that the computational time of TOPP-RA is comparable with Algorithm 1 using simplex method to solve the two-dimensional LP subproblems (41) (actually higher, since TOPP-RA solves $3n$ LP problems, while our approach solves only n LP problems).

5.3 Experimental results

This section presents an experiment on a minimum-time trajectory tracking task with a 6-DoF Mitsubishi RV-3SDB industrial robotic arm (see Figure 7). We require the end-effector to track an assigned path. To this end, we compute a corresponding trajectory Γ in the joint space and optimize the speed law on Γ by solving Problem 5 with Algorithm 1, using Algorithm 3 to solve the LP subproblems (41).

The reference path of the end-effector is generated using V-REP robot simulator software [7]. The path is defined by a Bezier curve with 6 control points (see Table 3). In the next step, the Bezier curve is sampled in 100 points (see Figure 8), which are transformed to joint space using an inverse kinematics method implemented in Robotics Toolbox for Matlab [4]. The obtained configurations in joint space are interpolated by a cubic spline, obtaining the reference path γ . Derivatives γ' , γ'' are calculated analytically from the spline coefficients. The reference path is sampled in $n = 1000$ points.

The following velocity and acceleration constraints are used for the six joints of the robot: ($\forall s \in [0, s_f]$)

$$\psi(s) = [1.0, \dots, 1.0]^T,$$

$$\alpha(s) = [4.0, \dots, 4.0]^T.$$

We implemented Algorithm 1 in C++. Velocity profile calculation takes less than $250 \mu s$. Figure 11 shows the generated velocity profile.

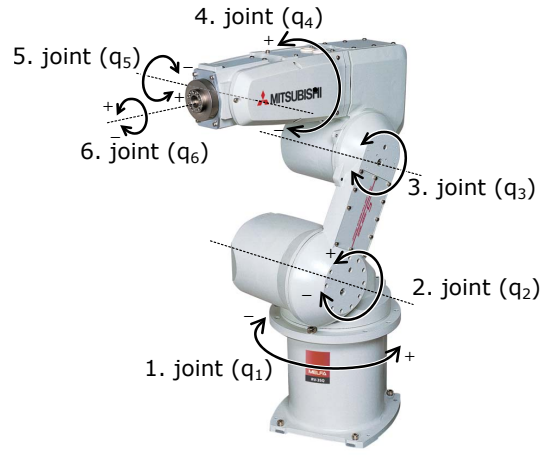


Figure 7: Mitsubishi RV-3SDB robot manipulator [13] ($\mathbf{q} = [q_1, q_2, q_3, q_4, q_5, q_6]^T$).

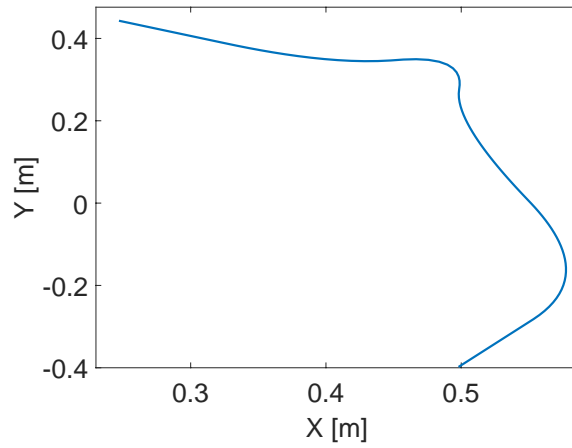


Figure 8: The reference path in the X-Y space.

Table 3: The control points of the path in V-REP.

X[m]	Y[m]	Z[m]
0.247	0.443	0.737
0.402	0.335	0.704
0.502	0.360	0.654
0.495	0.195	0.618
0.603	-0.178	0.537
0.498	-0.398	0.537

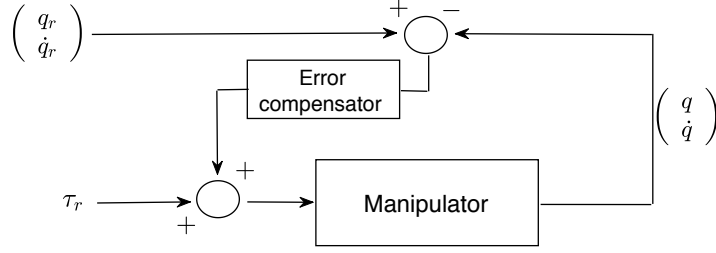


Figure 9: Standard tracking control scheme.

In order to compute a reference trajectory $(\mathbf{q}_r, \dot{\mathbf{q}}_r) : [0, s_f] \rightarrow T\mathcal{Q}$ and a reference input torque $\boldsymbol{\tau}_r : [0, s_f] \rightarrow \mathbb{R}^p$ the following procedure can be applied. After the discretized Problem 5 is solved, the continuous time functions $\boldsymbol{\tau}_c = \mathcal{I}\boldsymbol{\tau}$ and $b_c = \mathcal{I}b$ are obtained interpolating $\boldsymbol{\tau}$ and b as in Proposition 2. Then, the position function $\lambda : [0, t_f] \rightarrow [0, s_f]$ is computed as the solution of the differential equation

$$\begin{aligned}\dot{\lambda}(t) &= \sqrt{b_c(\lambda(t))} \\ \lambda(0) &= 0.\end{aligned}$$

Finally, the reference trajectory and input are defined as

$$\begin{aligned}\mathbf{q}_r(t) &= \boldsymbol{\gamma}(\lambda(t)), \\ \dot{\mathbf{q}}_r(t) &= \boldsymbol{\gamma}'(\lambda(t))\dot{\lambda}(t), \\ \boldsymbol{\tau}_r(t) &= \boldsymbol{\tau}_c(\lambda(t)).\end{aligned}$$

Then, one can achieve asymptotic exact tracking by the standard state tracking control scheme shown in Figure 9, in which the reference torque $\boldsymbol{\tau}_r$ enters as a feedforward control signal. Due to the limitations of the available hardware, we used a simplified control scheme. Namely, the implemented controller is a simple position setpoint regulator, where \mathbf{q}_r is used as a time-varying position reference signal (see Figure 10).

In particular, the robot is controlled using Mitsubishi Real-time external control capability [14]. In this control scheme, the robot controller receives the time-varying setpoint position \mathbf{q}_r from a PC via Ethernet communication. The controller sends back to the PC various monitor data (e.g., measured joint position, motor current). The controller sample rate is 7.1 ms [14].

Figure 12 shows the difference between the measured and the reference velocity profile for the second joint, while Figure 13 shows the joint position error for the same joint. Note that the tracking error is low despite the use of such a simple controller.

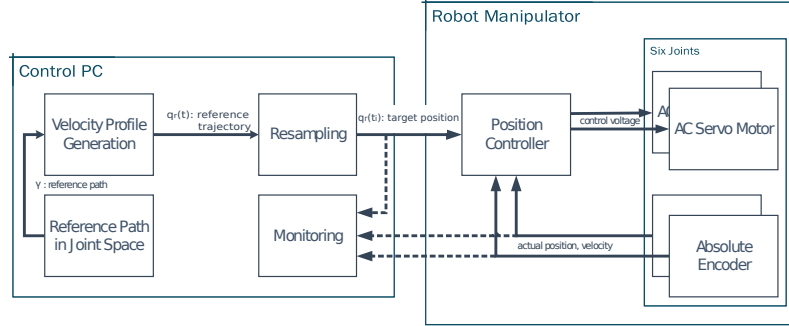


Figure 10: The implemented control scheme for trajectory tracking.

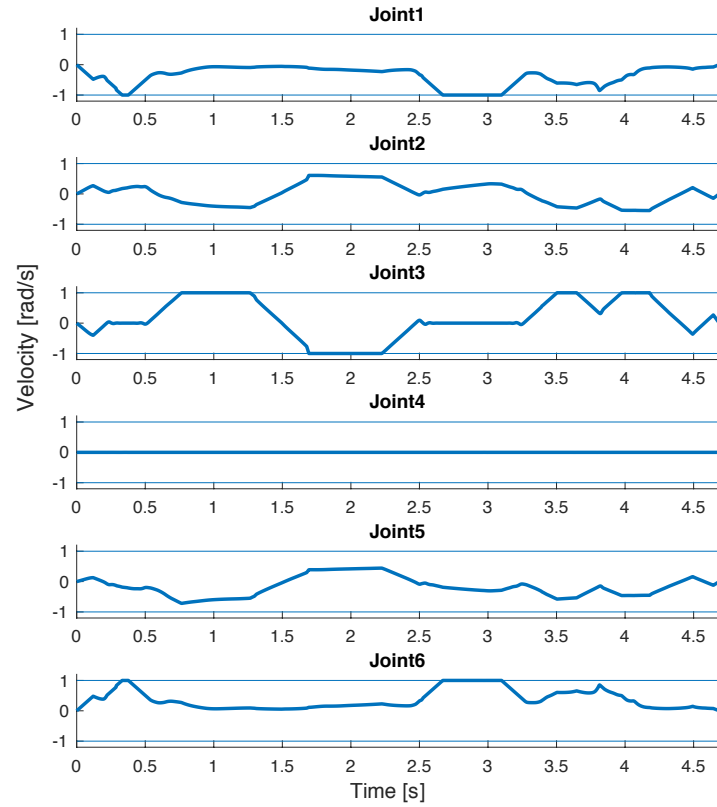


Figure 11: The generated profiles for the six-joints.

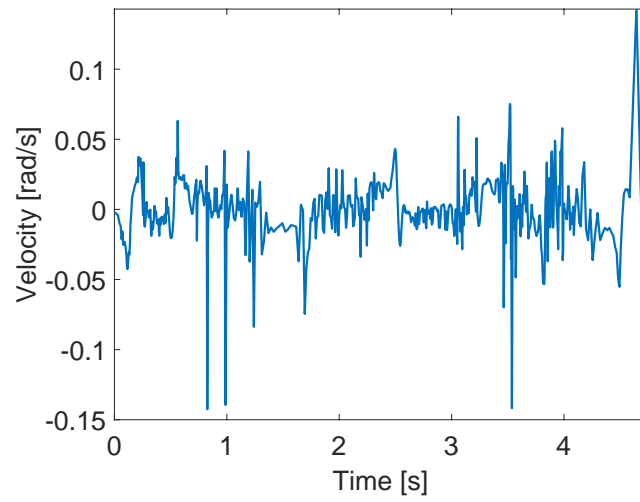


Figure 12: Measured velocity error for the second joint.

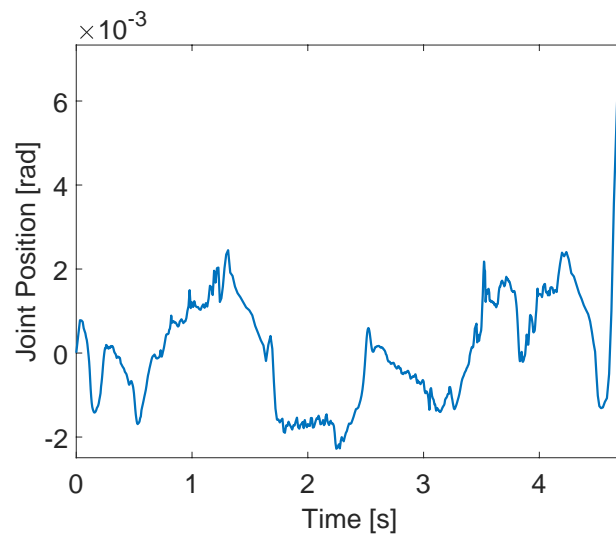


Figure 13: Measured joint position error for the second joint.

6 Conclusions

We solved a speed planning problem for the robot manipulators taking into account velocity, acceleration and torque constraints.

We proposed an algorithm which solves a class of optimization problems and we showed that, in case of linear constraints, the complexity of such algorithm is optimal.

Using a suitable discretization strategy we proved that the speed planning problem for robotic manipulators falls in the class of problems we introduced and that can be solved using the proposed algorithm.

By numerical experiments, we showed that the proposed algorithm solves the speed planning problem much faster than the other solvers proposed in the literature. Finally, we applied the proposed algorithm to control a real 6-DOF manipulator.

7 Appendix

7.1 Proof of Proposition 1

Let \mathcal{D} be the subset of $C^1([0, s_f], \mathbb{R})$ that satisfies conditions (19)-(25). Set $f(b) = \int_0^{s_f} b(s)^{-1/2} ds$ and $f^* = \inf\{f(b) : b \in \mathcal{D}\}$, then there exists a sequence of $b_i : [0, s_f] \rightarrow \mathbb{R}$, $i \in \mathbb{N}$, such that $b_i \in \mathcal{D}$ and $\lim_{i \rightarrow \infty} f(b_i) = f^*$. By Ascoli-Arzelà theorem, if the sequence $\{b_i\}$ is uniformly bounded and differentiable with $\{b'_i\}$ uniformly bounded, then there exists a subsequence $\{b_{i_k}\}$ that uniformly converges on $[0, s_f]$. Since $(\forall s \in [0, s_f]) \|\gamma'(s)\| = 1$, there exists an index $i(s) \in \{1, \dots, p\}$ such that $\gamma'_{i(s)}(s)^2 \geq \frac{1}{p}$. Then, we define a function $\beta : [0, s_f] \rightarrow \mathbb{R}_+$ as the most restrictive upper bound of b along the path. Hence, from constraint (23) we can write the following relation

$$0 \leq b(s) \leq \beta(s). \quad (67)$$

Since each function b_i is uniformly bounded (by (23) and boundedness of β) and differentiable, it remains to show that b'_i is uniformly bounded (i.e., there exists a real constant C such that, $\forall s \in [0, s_f]$, $|b'_i(s)| \leq C$). Consider constraint (24)

$$-2(\alpha(s) + \gamma''(s)b(s)) \leq \gamma'(s)b'(s) \leq 2(\alpha(s) - \gamma''(s)b(s)).$$

Since α and β are bounded functions, $\bar{\alpha} = \|\alpha\|_\infty < +\infty$ and $\bar{\beta} = \|\beta\|_\infty < +\infty$. Moreover, γ'' is a continuous function on the compact set $[0, s_f]$, then there exists the component-wise maximum $\bar{\gamma}'' = \|\gamma''\|_\infty$. Hence, we bound $\gamma'(s)b'(s)$ as follows

$$-2(\bar{\alpha} + \bar{\gamma}''\bar{\beta})\mathbf{1} \leq \gamma'(s)b'(s) \leq 2(\bar{\alpha} + \bar{\gamma}''\bar{\beta})\mathbf{1}.$$

Since $\forall s \in [0, s_f]$ $\|\gamma'(s)\|_2 = 1$, then there exists an index $i(s) \in \{1, \dots, p\}$ such that $\|\gamma'_{i(s)}(s)\|_\infty \geq \frac{1}{\sqrt{p}}$, which implies

$$-2\sqrt{p}(\bar{\alpha} + \bar{\gamma}''\bar{\beta}) \leq -2 \frac{(\bar{\alpha} + \bar{\gamma}''\bar{\beta})}{\|\gamma'_{i(s)}(s)\|_\infty} \leq b'(s) \leq \frac{(\bar{\alpha} + \bar{\gamma}''\bar{\beta})}{\|\gamma'_{i(s)}(s)\|_\infty} \leq 2\sqrt{p}(\bar{\alpha} + \bar{\gamma}''\bar{\beta}).$$

Hence, $|b'|$ is uniformly bounded by the real constant $C = 2\sqrt{p}(\bar{\alpha} + \bar{\gamma}''\bar{\beta})$.

To show that $f^*(b) \leq U < +\infty$, where U is a constant depending on the problem data, it is sufficient to find $b \in \mathcal{D}$ such that $f(b) < +\infty$. To this end, set for $\delta \geq 0$

$$b_\delta(s) = \begin{cases} \delta s(2\delta - s), & s \in [0, \delta], \\ \delta^3, & s \in [\delta, s_f - \delta], \\ \delta(s_f - s)(s - s_f + 2\delta), & s \in (s_f - \delta, s_f]. \end{cases}$$

Its derivative is

$$b'_\delta(s) = \begin{cases} 2\delta(\delta - s), & s \in [0, \delta], \\ 0, & s \in [\delta, s_f - \delta], \\ 2\delta(s_f - s - \delta), & s \in (s_f - \delta, s_f]. \end{cases}$$

Note that (25) is obviously satisfied by b_δ , moreover, $b_\delta \in \mathcal{D}$ if $\delta = 0$.

The maximum value of b_δ is δ^3 . By Assumption 1, there exists the minimum $\hat{\psi} = \min_{i=1,\dots,p} \min\{\psi_i(s) : s \in [0, s_f]\} > 0$. Since $\gamma \in C^2([0, s_f], \mathbb{R}^p)$ it follows that $\hat{\gamma}' = \|\gamma'\|_\infty^2 < +\infty$. Hence, setting $\hat{\delta} = (\hat{\psi}/\hat{\gamma}')^{\frac{2}{3}}$, (23) is satisfied for any $\delta \in [0, \hat{\delta}]$. After that, we have that ($\forall s \in [0, s_f]$)

$$\begin{aligned} & \left| \frac{1}{2} \mathbf{d}(s) b'_\delta(s) + \mathbf{c}(s) b_\delta(s) + \mathbf{g}(s) \right| \leq \\ & \leq \frac{1}{2} |\mathbf{d}(s)| |b'_\delta(s)| + |\mathbf{c}(s)| b_\delta(s) + |\mathbf{g}(s)|. \end{aligned}$$

By Assumption 2 it follows that

$$\begin{aligned} & \frac{1}{2} |\mathbf{d}(s)| |b'_\delta(s)| + |\mathbf{c}(s)| b_\delta(s) + |\mathbf{g}(s)| < \\ & < \frac{1}{2} |\mathbf{d}(s)| |b'_\delta(s)| + |\mathbf{c}(s)| b_\delta(s) + \boldsymbol{\mu}(s) - \varepsilon \mathbf{1}. \end{aligned}$$

There exists $\bar{\delta} > 0$ such that ($\forall s \in [0, s_f]$)

$$\frac{1}{2} |\mathbf{d}(s)| |b'_\delta(s)| + |\mathbf{c}(s)| b_\delta(s) \leq \varepsilon \mathbf{1},$$

which implies that for any $\delta \in [0, \bar{\delta}]$

$$\left| \frac{1}{2} \mathbf{d}(s) b'_\delta(s) + \mathbf{c}(s) b_\delta(s) + \mathbf{g}(s) \right| \leq \boldsymbol{\mu}(s),$$

i.e., b_δ satisfies constraints (22). Analogously one can see that constraint (24) is fulfilled for each $\delta \in [0, \bar{\delta}]$ with a sufficiently small $\bar{\delta} > 0$. Hence, for each $\delta \in [0, \delta^*]$ with $\delta^* = \min\{\hat{\delta}, \bar{\delta}, \tilde{\delta}\}$, it follows that $b_\delta \in \mathcal{D}$. Finally, by direct computation, it is straightforward to see that $f(b_\delta) < +\infty$, with $\delta > 0$. \square

7.2 Proof of Proposition 2

For $i = 2, \dots, n-1$, x_i, y_i, z_i need satisfy conditions

$$\begin{aligned} x_i - \frac{h}{2} y_i + \frac{h^2}{4} z_i &= b_{i-1/2}, \\ x_i + \frac{h}{2} y_i + \frac{h^2}{4} z_i &= b_{i+1/2}, \\ y_i - h z_i &= \delta_{i-1/2}, \\ y_i + h z_i &= \delta_{i+1/2}. \end{aligned} \tag{68}$$

Note that the last equation is redundant since it is a linear combination of the first three (with coefficients -1, +1, and $-h/2$, respectively). Conditions (68) can then be rewritten as

$$M \begin{pmatrix} x_i \\ y_i \\ z_i \end{pmatrix} = \begin{pmatrix} b_{i-1/2} \\ b_{i+1/2} \\ \delta_{i-1/2} \end{pmatrix}, \quad (69)$$

where

$$M = \begin{pmatrix} 1 & -\frac{h}{2} & \frac{h^2}{4} \\ 1 & \frac{h}{2} & \frac{h^2}{4} \\ 0 & 1 & -h \end{pmatrix}.$$

The solution of (68) (unique since M is nonsingular) is

$$\begin{aligned} x_i &= \frac{6b_i + b_{i-1} + b_{i+1}}{8} \\ y_i &= \frac{b_{i+1} - b_{i-1}}{2h} \\ z_i &= \frac{b_{i+1} + b_{i-1} - 2b_i}{2h^2}. \end{aligned} \quad (70)$$

Moreover x_1, y_1, z_1 need satisfy

$$\begin{aligned} x_1 &= b_1, \\ x_1 + \frac{h}{2}y_1 + \frac{h^2}{4}z_1 &= b_{1+1/2}, \\ y_1 + hz_1 &= \delta_{1+1/2}, \end{aligned}$$

whose solution is unique and is given by $x_1 = b_1, z_1 = 0, y_1 = \frac{b_2 - b_1}{2h}$. Finally, x_n, y_n, z_n need satisfy

$$\begin{aligned} x_n &= b_n, \\ x_n - \frac{h}{2}y_n + \frac{h^2}{4}z_n &= b_{n-1/2}, \\ y_n + hz_n &= \delta_{n-1/2}, \end{aligned}$$

whose solution is unique and is given by $x_n = b_n, z_n = 0, y_n = \frac{b_n - b_{n-1}}{h}$. \square

7.3 Proof of Proposition 8

Since the objective function (55) is monotonic non increasing and the variables $b_i, i = 0, \dots, n$, are non negative and bounded by (67), we only need to prove that constraints (64) and (62) satisfy Assumption 3 for suitable choices of $\lambda_{j,i}$ and $\eta_{i,j}, j = 1, \dots, p$ and $i = 1, \dots, n$.

For the sake of simplicity consider the j -th component of the i -th sample of (62). Substituting variable a_i and τ_i with (61) and (59) in constraints (62) we have:

$$|(d_{j,i} + 2hc_{j,i}\lambda_{j,i})b_{i+1} + (-d_{j,i} + (1 - \lambda_{j,i})2hc_{j,i})b_i + 2hg_{j,i}| \leq 2h\mu_{j,i}$$

First, we discuss the cases when $d_{j,i} = 0$ or $c_{j,i} = 0$. For these cases we set $\lambda_{j,i} = 1$. If $d_{j,i} = c_{j,i} = 0$, we have $|g_{j,i}| < \mu_{j,i}$ that is always true by Assumption 2. If $d_{j,i} = 0$ and $c_{j,i} \neq 0$ we have $|c_{j,i}b_{i+1} + g_{j,i}| \leq \mu_{j,i}$ that, after combining it with constraints (63), becomes $0 \leq b_{i+1} \leq \min\{\psi_{i+1}^2/\gamma_{j,i+1}^2, (\mu_{j,i} - g_{j,i})/|c_{j,i}|\}$. Finally, if $d_{j,i} \neq 0$ and $c_{j,i} = 0$ we have $|d_{j,i}(b_{i+1} - b_i) + 2hg_{j,i}| \leq 2h\mu_{j,i}$ that satisfies Assumption 3. If $d_{j,i} \neq 0$ and $c_{j,i} \neq 0$ we have:

$$-2h(\mu_{j,i} + g_{j,i}) \leq (d_{j,i} + 2hc_{j,i}\lambda_{j,i})b_{i+1} + (-d_{j,i} + (1 - \lambda_{j,i})2hc_{j,i})b_i \leq 2h(\mu_{j,i} - g_{j,i}).$$

In order to satisfy Assumption 3 we choose the value of $\lambda_{j,i}$ such that $(d_{j,i} + 2hc_{j,i}\lambda_{j,i})(-d_{j,i} + (1 - \lambda_{j,i})2hc_{j,i}) < 0$. Hence, we set

$$\lambda_{j,i} = \begin{cases} 1 & \text{if } d_{j,i}c_{j,i} > 0 \\ 0 & \text{if } d_{j,i}c_{j,i} < 0. \end{cases}$$

Using this selection technique we can rewrite constraint (59) as follows:

$$\tau_{j,i} = \begin{cases} d_{j,i}a_i + c_{j,i}b_{i+1} + g_{j,i}, & \text{if } d_{j,i}c_{j,i} > 0, \\ d_{j,i}a_i + c_{j,i}b_i + g_{j,i}, & \text{if } d_{j,i}c_{j,i} < 0. \end{cases}$$

Moreover, we can explicit constraints (62) in the form presented in (38). In fact, if $d_{j,i}c_{j,i} > 0$, the constraint (62) becomes:

$$\begin{aligned} b_{i+1} &\leq \frac{d_{j,i}}{d_{j,i} + 2hc_{j,i}}b_i + \left| \frac{2h(\mu_{j,i} - g_{j,i})}{d_{j,i} + 2hc_{j,i}} \right|, \\ b_i &\leq \frac{d_{j,i} + 2hc_{j,i}}{d_{j,i}}b_{i+1} + \left| \frac{2h(\mu_{j,i} + g_{j,i})}{d_{j,i}} \right| \end{aligned}$$

and, with $d_{j,i}c_{j,i} < 0$,

$$\begin{aligned} b_{i+1} &\leq \frac{d_{j,i} - 2hc_{j,i}}{d_{j,i}}b_i + \left| \frac{2h(\mu_{j,i} + g_{j,i})}{d_{j,i}} \right| \\ b_i &\leq \frac{d_{j,i}}{d_i - 2hc_{j,i}}b_{i+1} + \left| \frac{2h(\mu_{j,i} - g_{j,i})}{d_{j,i} - 2hc_{j,i}} \right|, \end{aligned}$$

which satisfy Assumption 3.

We use the same reasoning for constraints (64). Consider

$$|(\gamma'_{j,i} + 2h\gamma''_{j,i}\eta_{j,i})b_{i+1} + (-\gamma'_{j,i} + (1 - \eta_{j,i})2h\gamma''_{j,i})b_i| \leq 2h\alpha_{j,i}$$

Again, setting $\eta_{j,i} = 1$, we discuss the cases when $\gamma'_{j,i} = 0$ or $\gamma''_{j,i} = 0$. If $\gamma'_{j,i} = \gamma''_{j,i} = 0$, we have $|0| \leq \alpha_{j,i}$ that is always true. If $\gamma'_{j,i} = 0$ and $\gamma''_{j,i} \neq 0$ we have $|\gamma''_{j,i}b_i| \leq \alpha_{j,i}$ that becomes $0 \leq b_{i+1} \leq \alpha_{j,i}/|\gamma''_{j,i}|$. Finally, if $\gamma'_{j,i} \neq 0$ and $\gamma''_{j,i} = 0$ we have $|b_{i+1} - b_i| \leq 2h\alpha_{j,i}/|\gamma'_{j,i}|$ that satisfies Assumption 3. After that, with $\gamma'_{j,i} \neq 0$ and $\gamma''_{j,i} \neq 0$ we set

$$\eta_{j,i} = \begin{cases} 1 & \text{if } \gamma'_{j,i}\gamma''_{j,i} > 0 \\ 0 & \text{if } \gamma'_{j,i}\gamma''_{j,i} < 0, \end{cases}$$

which implies, for $\gamma'_{j,i} \cdot \gamma''_{j,i} > 0$:

$$\begin{aligned} b_{i+1} &\leq \frac{\gamma'_{j,i}}{\gamma'_{j,i} + 2h\gamma''_{j,i}}b_i + \left| \frac{2h\alpha_{j,i}}{\gamma'_{j,i} + 2h\gamma''_{j,i}} \right|, \\ b_i &\leq \frac{\gamma'_{j,i} + 2h\gamma''_{j,i}}{\gamma'_{j,i}}b_{i+1} + \left| \frac{2h\alpha_{j,i}}{\gamma'_{j,i}} \right|, \end{aligned}$$

and, with $\gamma'_{j,i} \cdot \gamma''_{j,i} < 0$,

$$\begin{aligned} b_{i+1} &\leq \frac{\gamma'_{j,i} - 2h\gamma''_{j,i}}{\gamma'_{j,i}} b_i + \left| \frac{2h\alpha_{j,i}}{\gamma'_{j,i}} \right| \\ b_i &\leq \frac{\gamma'_{j,i}}{\gamma'_{j,i} - 2h\gamma''_{j,i}} b_{i+1} + \left| \frac{2h\alpha_{j,i}}{\gamma'_{j,i} - 2h\gamma''_{j,i}} \right|. \end{aligned}$$

which satisfy Assumption 3. □

References

- [1] J.E. Bobrow, S. Dubowsky, and J.S. Gibson. Time-optimal control of robotic manipulators along specified paths. *The International Journal of Robotics Research*, 4(3):3–17, 1985.
- [2] Luca Consolini, Mattia Laurini, Marco Locatelli, and Federico Cabassi. Convergence analysis of spatial-sampling based algorithms for time-optimal smooth velocity planning. *submitted to Automatica*, 2017.
- [3] Luca Consolini, Marco Locatelli, Andrea Minari, and Aurelio Piazzzi. An optimal complexity algorithm for minimum-time velocity planning. *Systems & Control Letters*, 103:50 – 57, 2017.
- [4] Peter I. Corke. *Robotics, Vision and Control: Fundamental Algorithms in Matlab*. Springer, 2011.
- [5] Gábor Csorvási, Ákos Nagy, and István Vajk. Near time-optimal path tracking method for waiter motion problem. *IFAC-PapersOnLine*, 50(1):4929–4934, 2017.
- [6] Frederik Debruwre, Wannes Van Loock, Goele Pipeleers, Quoc Tran Dinh, Moritz Diehl, Joris De Schutter, and Jan Swevers. Time-optimal path following for robots with convex–concave constraints using sequential convex programming. *IEEE Transactions on Robotics*, 29(6):1485–1495, 2013.
- [7] M. Freese E. Rohmer, S. P. N. Singh. V-rep: A versatile and scalable robot simulation framework. In *Proc. of The International Conference on Intelligent Robots and Systems (IROS)*, 2013.
- [8] Inc. Gurobi Optimization. Gurobi optimizer reference manual, 2016.
- [9] Kris Hauser. Fast interpolation and time-optimization with contact. *The International Journal of Robotics Research*, 33(9):1231–1250, 2014.
- [10] Steven M. LaValle. *Planning Algorithms*. Cambridge University Press, New York, NY, USA, 2006.
- [11] Thomas Lipp and Stephen Boyd. Minimum-time speed optimisation over a fixed path. *International Journal of Control*, 87(6):1297–1311, 2014.

- [12] Nimrod Megiddo. Linear-time algorithms for linear programming in \mathbb{R}^3 and related problems. *SIAM Journal on Computing*, 12(4):759–776, 1983.
- [13] Mitsubishi. *RV-3SD/3SDJ/3SDB/3SDBJ Series: Standard Specifications Manual*, 2009.
- [14] Mitsubishi. *CR750/CR751 Series Controller Instruction Manual*, 2014.
- [15] Richard M Murray, Zexiang Li, and S Shankar Sastry. *A mathematical introduction to robotic manipulation*. CRC press, 1994.
- [16] Ákos Nagy and István Vajk. LP-based velocity profile generation for robotic manipulators. *International Journal of Control*, 91:582–592, 2018.
- [17] M. Oberherber, H. Gattringer, and A. Mller. Successive dynamic programming and subsequent spline optimization for smooth time optimal robot path tracking. *Mechanical Sciences*, 6(2):245–254, 2015.
- [18] Friedrich Pfeiffer and Rainer Johanni. A concept for manipulator trajectory planning. *IEEE Journal on Robotics and Automation*, 3(2):115–123, 1987.
- [19] Hung Pham and Quang-Cuong Pham. A new approach to time-optimal path parameterization based on reachability analysis. *arXiv preprint arXiv:1707.07239*, 2017.
- [20] Quang-Cuong Pham. A general, fast, and robust implementation of the time-optimal path parameterization algorithm. *IEEE Transactions on Robotics*, 30(6):1533–1540, 2014.
- [21] Quang-Cuong Pham, Stéphane Caron, and Yoshihiko Nakamura. Kinodynamic planning in the configuration space via velocity interval propagation. *Robotics: Science and System*, 2013.
- [22] Quang-Cuong Pham and Olivier Stasse. Time-optimal path parameterization for redundantly actuated robots: A numerical integration approach. *IEEE/ASME Transactions on Mechatronics*, 20(6):3257–3263, 2015.
- [23] Zvi Shiller and Hsueh-Hen Lu. Computation of path constrained time optimal motions with dynamic singularities. *Journal of Dynamic Systems, Measurement, and Control*, 114(1):34–40, 1992.
- [24] Kang Shin and N McKay. A dynamic programming approach to trajectory planning of robotic manipulators. *IEEE Transactions on Automatic Control*, 31(6):491–500, 1986.
- [25] S Singh and Ming-Chuan Leu. Optimal trajectory generation for robotic manipulators using dynamic programming. *Journal of Dynamic Systems, Measurement, and Control*, 109(2):88–96, 1987.
- [26] J. J. E. Slotine and H. S. Yang. Improving the efficiency of time-optimal path-following algorithms. *IEEE Transactions on Robotics and Automation*, 5(1):118–124, Feb 1989.
- [27] D. Verscheure, B. Demeulenaere, J. Swevers, J. De Schutter, and M. Diehl. Time-optimal path tracking for robots: A convex optimization approach. *IEEE Transactions on Automatic Control*, 54(10), Oct 2009.